

# Simple and Efficient Route to Prepare Homogeneous Samples of $\text{Sr}_2\text{FeMoO}_6$ with a High Degree of Fe/Mo Order

Y. H. Huang,<sup>†,‡</sup> J. Lindén,<sup>§</sup> H. Yamauchi,<sup>†</sup> and M. Karppinen<sup>\*,†</sup>

*Materials and Structures Laboratory, Tokyo Institute of Technology, 4259 Nagatsuta, Midori-ku, Yokohama 226-8503, Japan, and Physics Department, Åbo Akademi, FIN-20500 Turku, Finland*

*Received April 26, 2004. Revised Manuscript Received July 28, 2004*

Polycrystalline  $\text{Sr}_2\text{FeMoO}_6$  samples are synthesized by an encapsulation technique under very low oxygen partial pressures utilizing the Fe/FeO redox couple as an oxygen getter. A route based on thermal decomposition of metal complexes, using ethylenediaminetetraacetic acid as the complexant, is developed to prepare a precursor powder. Single-phase samples are readily obtained even at temperatures as low as 900 °C. The degree of Fe/Mo ordering and the grain size are well-controlled by sintering temperature and time. Homogeneous morphology of the samples is confirmed from scanning electron microscopy images. Rietveld refinements of X-ray diffraction patterns indicate that the degree of order ( $S$ ) at the Fe/Mo sites is higher than 0.95 for samples sintered at 1150 °C for 100 h. For the same sample a record-high saturation magnetization of  $3.96 \mu_{\text{B}}$ , which is very close to the theoretical value of  $4 \mu_{\text{B}}$ , is obtained. It is considered that the high degree of order stems from the uniform mixing of starting reactants in an atomic scale and also from the stability of overall cation stoichiometry during sample sintering in an encapsulated ampule. It is found that the Curie temperature exhibits a nonmonotonic dependence on  $S$ , with the maximum at  $S \approx 0.84$ . Additionally, evidence for super-paramagnetic-type behavior in the present solution-derived samples is obtained from the Mössbauer data.

## Introduction

Due to its remarkable tunneling-type magnetoresistance (TMR) effect achieved even at room temperature and low applied magnetic fields, the  $\text{A}_2\text{BB}'\text{O}_6$ -type double-perovskite,  $\text{Sr}_2\text{FeMoO}_6$ , has drawn a great deal of attention.<sup>1</sup> It is considered that in  $\text{Sr}_2\text{FeMoO}_6$  a long-range magnetic interaction between the spins of the B-site cation constituents,  $\text{Fe}^{\text{II/III}}$  ( $S = 5/2$ ) and  $\text{Mo}^{\text{V}}$  ( $S = 1/2$ ), can induce a ferrimagnetic half-metallic state with a large saturation magnetization ( $M_{\text{S}}$ ) of  $4 \mu_{\text{B}}$  per formula unit. As a consequence of the fact that the itinerant  $4d^1$  electron of the formally pentavalent Mo transfers part of its charge and spin to the formally trivalent Fe, both  $^{57}\text{Fe}$  Mössbauer<sup>2</sup> and Fe K- and L-edge XANES<sup>3</sup> data have indicated a mixed-valence state of II/III for Fe in  $\text{Sr}_2\text{FeMoO}_6$ . In line with the II/III valence state of Fe, an NMR study suggested a mixed-valence state of V/VI for Mo.<sup>4</sup> Even though  $4 \mu_{\text{B}}$  is expected for the  $M_{\text{S}}$  value, experimentally observed values typically

remain below  $3.7 \mu_{\text{B}}$ ,<sup>5,6</sup> and values exceeding  $3.9 \mu_{\text{B}}$ <sup>7</sup> have not been reported yet. (Note that the magnitude of  $M_{\text{S}}$  should not depend on the degree of valence mixing between  $\text{Fe}^{\text{II/III}}$  and  $\text{Mo}^{\text{V/VI}}$ .) It is well-documented that the lower-than-predicted  $M_{\text{S}}$  value is due to partial disorder within the B-cation sublattice, i.e., antisite (AS) defects.<sup>5,8</sup> From Mössbauer spectra for  $\text{Sr}_2\text{FeMoO}_6$ , the AS Fe atoms have been revealed to be trivalent. Their concentration is conveniently monitored by means of Mössbauer spectroscopy.

It has been suggested that the TMR effect is related to the Fe/Mo ordering such that the higher degree of order yields the larger magnetoresistance.<sup>9</sup> Thus, ways to increase the degree of order in the B-cation sublattice of  $\text{Sr}_2\text{FeMoO}_6$  are needed for both technological and fundamental considerations. Thermodynamically the lower the synthesis temperature is, the higher the degree of order should be.<sup>7</sup> However, at low temperatures cation diffusion is extremely slow such that the

\* Corresponding author. Phone: +81-45-924-5333. Fax: +81-45-924-5365. E-mail: karppinen@mssl.titech.ac.jp.

<sup>†</sup> Tokyo Institute of Technology.

<sup>‡</sup> Permanent address: Institute of Advanced Materials, Fudan University, Shanghai 200433, China.

<sup>§</sup> Åbo Akademi.

(1) Kobayashi, K.-I.; Kimura, T.; Sawada, H.; Terakura, K.; Tokura, Y. *Nature (London)* **1998**, *395*, 677.

(2) Lindén, J.; Yamamoto, T.; Karppinen, M.; Yamauchi, H.; Pietari, T. *Appl. Phys. Lett.* **2000**, *76*, 2925.

(3) Karppinen, M.; Yamauchi, H.; Yasukawa, Y.; Lindén, J.; Chan, T. S.; Liu, R. S.; Chen, J. M. *Chem. Mater.* **2003**, *15*, 4118.

(4) Kapusta, Cz.; Riedi, P. C.; Zajac, D.; Sikora, M.; De Teresa, J. M.; Morellon, L.; Ibarra, M. R. *J. Magn. Magn. Mater.* **2002**, *242–245*, 701.

(5) Balcells, Ll.; Navarro, J.; Bibes, M.; Roig, A.; Martínez, B.; Fontcuberta, J. *Appl. Phys. Lett.* **2001**, *78*, 781.

(6) Navarro, J.; Nogués, J.; Muñoz, J. S.; Fontcuberta, J. *Phys. Rev. B* **2003**, *67*, 174416.

(7) Shimada, T.; Nakamura, J.; Motohashi, T.; Yamauchi, H.; Karppinen, M. *Chem. Mater.* **2003**, *15*, 4494.

(8) Ogale, A. S.; Ogale, S. B.; Ramesh, R.; Venkatesan, T. *Appl. Phys. Lett.* **1999**, *75*, 537.

(9) García-Hernández, M.; Martínez-Lope, J. L.; Casais, M. T.; Alonso, J. A. *Phys. Rev. Lett.* **2001**, *86*, 2443.

degree of order is rather limited by kinetics.<sup>7</sup> The most commonly employed synthesis route for the Sr<sub>2</sub>FeMoO<sub>6</sub> phase involves firing of mechanically mixed powder precursors in flowing H<sub>2</sub>/Ar or H<sub>2</sub>/N<sub>2</sub> gas at 900–1200 °C.<sup>1,5</sup> The drawback of this method is that once one aims at samples with a high degree of Fe/Mo order the very long heating periods that are required to complete the cation diffusion are likely to yield cation-nonstoichiometric samples due to partial evaporation of some of the constituent metals. Impurity phases of SrMoO<sub>4</sub> and SrFeO<sub>3-δ</sub> commonly appear in such samples. Moreover, application of H<sub>2</sub>-containing gas flow brings about the need to pay extra attention to experimental safety. Some efforts to shorten the required heating periods by employing sol–gel routes to obtain homogeneous precursors have been reported.<sup>10,11</sup> In these studies sintering was carried out under H<sub>2</sub>/N<sub>2</sub> gas flow, and thus impurities such as SrMoO<sub>4</sub> were still observed. We recently introduced an encapsulation technique utilizing iron as an oxygen getter to prepare high-quality Sr<sub>2</sub>-FeMoO<sub>6</sub> samples.<sup>7,12</sup> This technique not only makes the preparation procedure safe and simple but also efficiently prevents the volatilization of the constituent metals during the (long) sintering period. Here we further improved this encapsulation technique by using a wet-chemistry route for preparing a homogeneous precursor powder, such that the formation of the Sr<sub>2</sub>-FeMoO<sub>6</sub> phase and the ordering of cations are facilitated more efficiently. Using a solution-homogenized powder as the precursor, an almost completely ordered sample with a record-high  $M_S$  value of 3.96  $\mu_B$  was obtained.

### Experimental Section

The precursor powder for Sr<sub>2</sub>FeMoO<sub>6</sub> was prepared by thermal decomposition of a complex gel obtained using ethylenediaminetetraacetic acid (EDTA) as a complexant. Stoichiometric amounts of SrCO<sub>3</sub>, Fe(NO<sub>3</sub>)<sub>3</sub>·9H<sub>2</sub>O, and (NH<sub>4</sub>)<sub>6</sub>Mo<sub>7</sub>O<sub>24</sub>·4H<sub>2</sub>O were dissolved in a diluted nitric acid aqueous solution. The molar ratio between the total amount of metal ions and the amount of EDTA was 1:1.5. The acidic solution containing the metal ions was added in drops into an NH<sub>4</sub>–EDTA solution, while being stirred at ambient temperature. Ammonia and nitric acid were used to adjust the pH value to ~9 to achieve a clear deep-purple solution. After heating this solution at ~200 °C, an amorphous gel was formed. The gel ignited spontaneously to turn into a raw ash when the excess free water evaporated. The ash was calcined in air at 900 °C for 15 h to obtain the precursor powder for the encapsulation synthesis. The precursor powder was pelletized and subsequently encapsulated into an evacuated fused-quartz ampule containing Fe grains (≥99.9%, under 10 mesh) to act as a getter for oxygen, as described in our previous works.<sup>7,12</sup> The sample ampule was fired at different temperatures ( $T_s$ ) ranging from 900 to 1150 °C. Also the sintering period ( $t_s$ ) was varied. In the employed temperature range the oxygen partial pressure inside the ampule in the presence of the Fe/FeO redox couple is estimated at 10<sup>-13</sup>–10<sup>-17</sup> atm.<sup>13</sup>

The phase purity and the lattice parameters were checked by X-ray powder diffraction (XRD; Cu K $\alpha$  radiation). The diffraction profiles were analyzed using a Rietveld refinement

program, RIETAN 2000.<sup>14</sup> All the patterns were refined in tetragonal space group,  $I4/m$ .<sup>15,16</sup> The degree of B-cation order was calculated as  $S = 2(g_{Fe} - 0.5)$  from the refined occupancy of Fe at its correct site ( $g_{Fe}$ ). Micrographs were taken for the samples by a scanning electron microscope (SEM; Hitachi: S4500). Magnetic measurements were performed using a superconducting quantum interference device (SQUID; Quantum Design: MPMS-XL5) and a vibrating sample magnetometer (VSM; Lakeshore VSM 7300).

For the <sup>57</sup>Fe Mössbauer measurement an absorber was made of the sample sintered at 1150 °C for 100 h by spreading a portion of the sample powder, mixed with an epoxy resin, on an Al foil. The absorber thickness was ~20 mg/cm<sup>2</sup>. For the second measurement under a magnetic field the sample was cut into rectangular shape of 6 mm × 20 mm and inserted between the poles of two permanent Nd–Fe–B magnets. The direction of the field was parallel to the shorter edge of the rectangle, and the field strength was approximately 600 mT. The field was homogenized using an external “horseshoe” of soft iron. Both spectra were recorded in a transmission geometry using the maximum Doppler velocity of 11.15 mm/s. The absorber temperature was set at 77 K. A Cyclotron Co. <sup>57</sup>Co:Rh (25 mCi, Jan. 2002) source was used. The direction of the  $\gamma$ -rays was perpendicular to the external magnetic field. The full Hamiltonian of combined electric and magnetic interactions was used to fit the spectra, with the total magnetic field experienced by the Fe nucleus ( $B$ ), the chemical isomer shift relative to  $\alpha$ -Fe at 300 K ( $\delta$ ), the quadrupole coupling constant ( $eQV_{zz}$ ), the resonance line widths ( $\Gamma$ ), and the relative intensities of the components ( $I$ ) as fit parameters. For each component a certain variation in the parameter  $B$  was allowed in order to simulate the fact that the internal fields have a certain spread: a Gaussian distribution was assumed, and its width ( $\Delta B$ ) was also introduced as a fit parameter.

### Results and Discussion

High-quality precursor powders were readily obtained by the EDTA-based complexing method. Since EDTA is a strong complexing agent, it quickly reacts with Sr<sup>2+</sup>, Fe<sup>3+</sup>, and Mo<sup>6+</sup> to form a complex at pH ≈ 9. Moreover, EDTA serves as an efficient fuel, producing a large quantity of heat to directly crystallize the oxide phase from the molecular mixture of the precursor solution. Previously it was demonstrated that EDTA is decomposed almost completely when the temperature reaches 500 °C.<sup>17</sup> In Figure 1, shown are XRD patterns for precursor powders which were calcined at 700, 800, and 900 °C. After calcination at 700 °C, the precursor powder consists of two main phases, SrMoO<sub>4</sub> (JCPDS No. 80-0842) and SrFeO<sub>3-δ</sub> (JCPDS No. 34-0641). The Sr<sub>2</sub>FeMoO<sub>6</sub> phase appears in precursors calcined at 800 °C and higher temperatures. For powders calcined at 800 or 900 °C three main phases are seen: SrMoO<sub>4</sub>, SrFeO<sub>3-δ</sub>, and Sr<sub>2</sub>FeMoO<sub>6</sub>. We found that the precursors calcined at 800 and 900 °C more efficiently facilitated the formation of the Sr<sub>2</sub>FeMoO<sub>6</sub> phase during the encapsulation synthesis as compared with the 700 °C-calcined precursor. Therefore, for the further experiments all the precursor powders used were calcined at 900 °C.

Figure 2 shows XRD patterns with intensities in logarithmic scale for samples sintered at different

(10) Yuan, C. L.; Wang, S. G.; Song, W. H.; Yu, T.; Dai, J. M.; Ye, S. L.; Sun, Y. P. *Appl. Phys. Lett.* **1999**, *75*, 3853.

(11) Song, W. H.; Dai, J. M.; Ye, S. L.; Wang, K. Y.; Du, J. J.; Sun, Y. P. *J. Appl. Phys.* **2001**, *89*, 7678.

(12) Yamamoto, T.; Liimatainen, J.; Lindén, J.; Karppinen, M.; Yamauchi, H. *J. Mater. Chem.* **2000**, *10*, 2342.

(13) Richardson, F. D.; Jeffes, J. H. E. *J. Iron Steel Inst. London* **1948**, *160*, 261.

(14) Izumi, F.; Ikeda, T. *Mater. Sci. Forum* **2000**, *321*, 198.

(15) Woodward, P. M. *Acta Crystallogr., Sect. B: Struct. Sci.* **1997**, *53*, 32.

(16) Chmaissem, O.; Kruk, R.; Dabrowski, B.; Brown, D. E.; Xiong, X.; Kolesnik, S.; Jorgensen, J. D.; Kimball, C. W. *Phys. Rev. B* **2000**, *62*, 14197.

(17) Huang, Y. H.; Xu, Z. G.; Yan, C. H.; Wang, Z. M.; Zhu, T.; Liao, C. S.; Gao, S.; Xu, G. X. *Solid State Commun.* **2000**, *114*, 43.

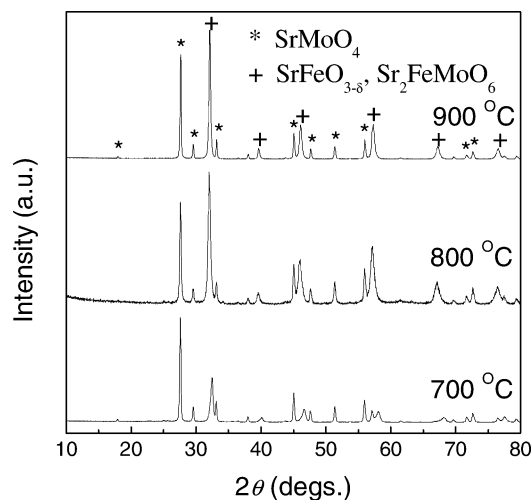


**Figure 1.** XRD patterns for the precursor powders calcined at different temperatures for 15 h.

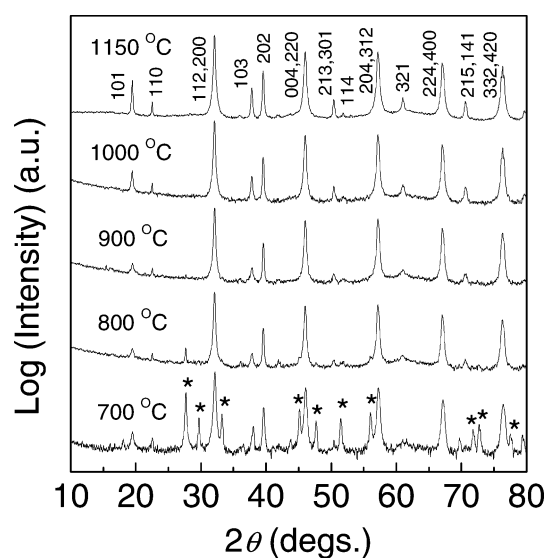


**Figure 2.** XRD patterns with intensities in logarithmic scale for  $\text{Sr}_2\text{FeMoO}_6$  samples sintered at different temperatures for 24 h. The asterisks represent the peaks of  $\text{SrMoO}_4$ .

temperatures,  $T_s$ , for 24 h. It is seen that only the 700 °C-sintered sample contains larger amounts of  $\text{SrMoO}_4$  as an impurity. For the  $T_s = 800$  °C sample, a very tiny amount of  $\text{SrMoO}_4$  is observed. When  $T_s$  exceeds 900 °C, no peaks due to any impurity are detected. The pure  $\text{Sr}_2\text{FeMoO}_6$  phase is obtained at 900 °C even with a 4 h sintering period only. Here it seems that the fast phase formation is facilitated because the precursor powder already contains some preformed  $\text{Sr}_2\text{FeMoO}_6$  that serves as growing centers for further crystallization during the sintering process.

In Figure 3, SEM images for  $\text{Sr}_2\text{FeMoO}_6$  samples obtained at different sintering temperatures are shown. For  $T_s = 900$  °C ( $t_s = 24$  h), round grains with a diameter of about 0.1  $\mu\text{m}$  are observed. Some of them aggregate with each other. The size of the grains becomes larger and also the shape of them changes when  $T_s$  increases. For  $T_s = 1000$  °C ( $t_s = 50$  h), the grains are of cubic shape with a size of  $\sim 0.5$   $\mu\text{m}$ . When  $T_s = 1150$  °C, polyhedral grains with an average size of about 3  $\mu\text{m}$  are achieved for  $t_s = 50$  h, but the grain size increases very slowly with a further increase in  $t_s$ .

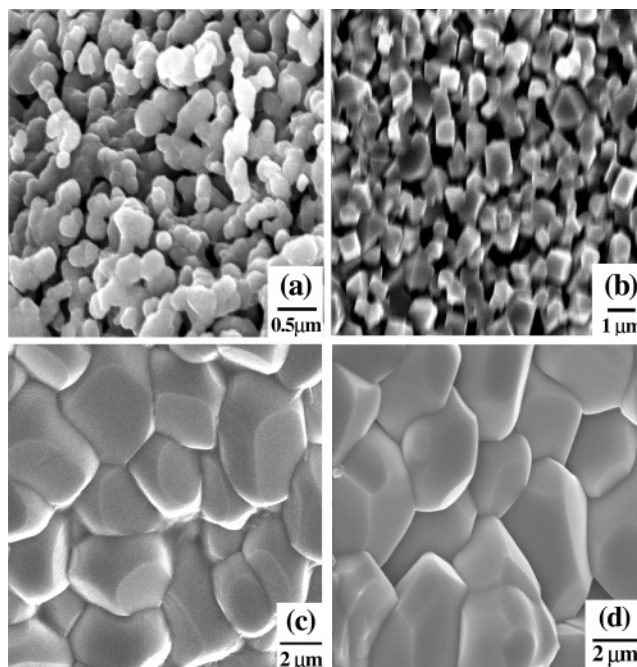


**Figure 3.** SEM images for  $\text{Sr}_2\text{FeMoO}_6$  samples obtained under different conditions: (a) 900 °C for 24 h, (b) 1000 °C for 50 h, (c) 1150 °C for 50 h, and (d) 1150 °C for 100 h.

From the sample morphology, all the present samples look highly homogeneous. The shape of the grains depends mainly on  $T_s$ . The gradual change in grain shape from the round one to a polyhedron indicates that sintering of the grains/crystallization becomes enhanced as  $T_s$  increases.

The degree of B-cation order,  $S$ , as calculated from Rietveld refinement results is greatly enhanced with increasing  $T_s$  within the investigated temperature range of 900–1150 °C (with  $t_s = 50$  h). On the other hand, at each  $T_s$ , increasing the sintering time causes  $S$  to increase. According to our previous work,<sup>7</sup> the optimum temperature range to achieve high- $S$  samples is about 1150 °C, because at  $\sim 1150$  °C the equilibrium value of  $S$  is close to unity: lowering the  $T_s$  below  $\sim 1150$  °C would not considerably enhance the equilibrium value of  $S$  but would make the sintering time required to achieve that value markedly longer. For  $T_s = 1150$  °C,  $S$  was found to be higher than 0.90 for the sample sintered for 4 h only, reached 0.94 for a sample sintered for 24 h, and exceeded 0.95 for the one sintered for 100 h. The degree of Fe/Mo order is much higher in the present case as compared with the samples prepared with the same encapsulation technique but using mechanically mixed precursor powders; see Figure 4. In fact, in the wet-chemical route the starting metal ions are mixed in an atomic scale, which enables us to achieve a homogeneous reaction system. In this case, the pure phase is readily formed, and Fe and Mo ions are distributed at the B- and B'-sites more strictly.

For some of the samples the degree of Fe/Mo order was checked on the basis of saturation magnetization as well. The theoretical relationship<sup>8</sup> between  $M_S$  and  $S$  has been derived as  $M_s = 4S$ . Figure 5 depicts magnetization ( $M$ ) as a function of applied field ( $H$ ) at 5 and 300 K for  $\text{Sr}_2\text{FeMoO}_6$  samples sintered at 1150 °C for different time periods. The  $M_S$  value is obtained

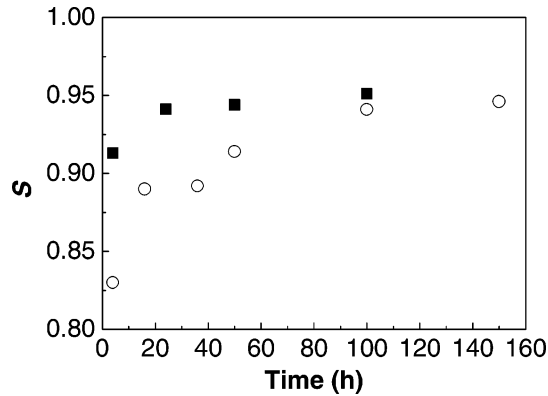


**Figure 4.** Dependence of sintering time on degree of order ( $S$ ) for  $\text{Sr}_2\text{FeMoO}_6$  samples fired at  $1150^\circ\text{C}$ . Solid squares are the data of the present work, and the open circles are for samples synthesized from mechanically mixed precursors in ref 7.

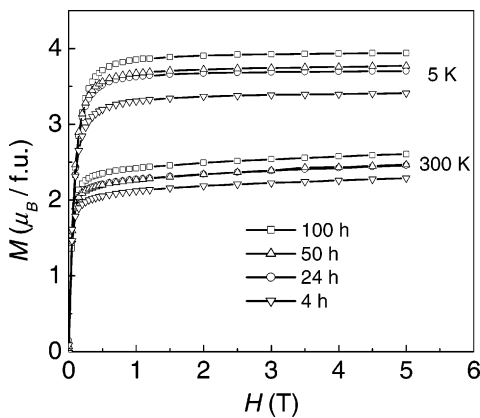


**Figure 5.** Magnetization as a function of applied field at 5 and 300 K for  $\text{Sr}_2\text{FeMoO}_6$  samples sintered at  $1150^\circ\text{C}$  for different times.

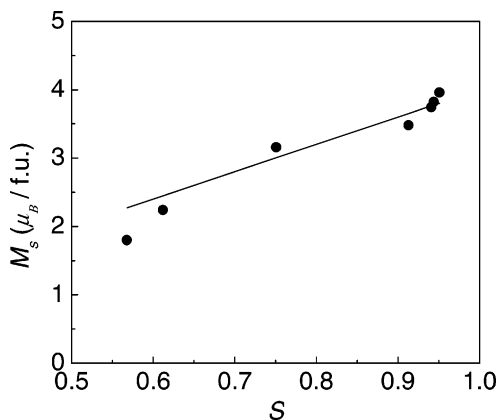


**Figure 6.** Saturation magnetization ( $M_s$ ) at 5 K as a function of degree of order ( $S$ ) for  $\text{Sr}_2\text{FeMoO}_6$  samples. The line represents the theoretical  $M_s$  values calculated by  $M_s = 4S$ .

from extrapolation of  $M$  vs  $1/H$  to  $1/H = 0$ . In Figure 6, we plot  $M_s$  as a function of  $S$ : it is seen that  $M_s$  increases with  $S$  roughly according to theory. However, the experimental  $M_s$  is lower than the theoretical one when  $S$  is small. This is because of the magnetic disorder in grain boundaries caused by incomplete crystallization at low  $T_s$ . Here, the striking feature is that a high  $M_s$  value can be obtained when  $T_s = 1150^\circ\text{C}$  even for a short sintering time. For example,  $M_s = 3.48 \mu_B$  for 4 h sintering, and  $M_s = 3.74 \mu_B$  for 24 h

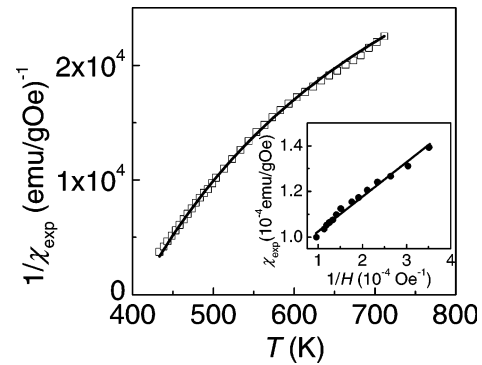


**Figure 7.** Temperature dependence of magnetic susceptibility (open symbols) at  $H = 0.7$  T for the sample sintered at  $1150^\circ\text{C}$  for 100 h. The line shows the fitness using an ordinary Curie–Weiss expression:  $\chi = C/(T - \theta_p) + A$ . The isothermal field dependence of the measured susceptibility at  $T = 500$  K is displayed in the inset.

sintering. Notably,  $M_s$  reaches  $3.96 \mu_B$  for a sample sintered at  $1150^\circ\text{C}$  for 100 h, which is close to the theoretical maximum. To our knowledge, this is the highest reported value of  $M_s$  for  $\text{Sr}_2\text{FeMoO}_6$ .

The record-low concentration of antite Fe and high  $M_s$  value for the sample sintered at  $1150^\circ\text{C}$  for 100 h deserves further studies. To do this, the paramagnetic susceptibility was measured up to 710 K in a field of 0.7 T. As shown in Figure 7, the thus-obtained data can be well-fitted by an ordinary Curie–Weiss expression:

$$\chi_{\text{exp}} = C/(T - \theta) + A \quad (1)$$

where the constant  $A$  accounts for the bending of the  $\chi_{\text{exp}}^{-1}$  curve, as explained further in the text. The fitted value of the Curie constant is  $C = 7.63 \times 10^{-3}$  Kemu/gOe, and the Weiss temperature  $\theta = 406.1$  K. An effective paramagnetic moment  $\mu_{\text{eff}}$  of  $5.1 \mu_B$  is obtained from  $C$ . This is less than expected for the  $3d^5$  (Fe) and  $4d^1$  (Mo) high-spin configuration, but slightly larger than that of a pure mixed-valence configuration of  $3d^{5.5}$  (Fe) and  $4d^{0.5}$  (Mo). In other words a certain degree of valence mixing is still present above  $T_C$ . This is in accordance with a Mössbauer study of paramagnetic samples.<sup>18</sup> The bending of the  $\chi_{\text{exp}}^{-1}$  vs  $T$  curve has been explained by temperature-induced delocalization of charge carriers.<sup>19</sup> However, the most logical explanation is the presence of tiny amounts of metallic Fe,<sup>20</sup> which is invisible to probing by X-ray diffraction or Mössbauer spectroscopy. The ferromagnetic moment of the Fe impurities is given by  $M_s(\text{Fe}) = AH$ , where  $A$  is the constant from expression (1). From the fitting of the data in Figure 7, we get an estimate of  $0.13$  emu/g for  $M_s(\text{Fe})$ . On the other hand, we can also obtain the value of  $M_s(\text{Fe})$  by a field scan, given in the inset of Figure 7. The field scan was recorded at 500 K in a maximum field of 1.1 T. According to expression (1), the experimental susceptibility is given by  $\chi_{\text{exp}} = (1-x)\chi(\text{Sr}_2\text{FeMoO}_6) + xM_s^\circ(\text{Fe})/H$ , where  $x$  is the fraction of impurity Fe and  $M_s^\circ(\text{Fe})$  is the saturation magnetiza-

(18) Lindén, J.; Yamamoto, T.; Nakamura, J.; Yamauchi, H.; Karppinen, M. *Phys. Rev. B* **2002**, *66*, 184408.

(19) Niebieskikwiat, D.; Sánchez, R. D.; Caneiro, A.; Morales, L.; Vázquez-Mansilla, M.; Rivadulla, F.; Hueso, L. E. *Phys. Rev. B* **2000**, *62*, 3340.

(20) Martínez, B.; Navarro, J.; Balcells, Ll.; Fontcuberta, J. J. *Phys.: Condens. Matter* **2000**, *12*, 10515.

tion of Fe. Thus,  $\chi_{\text{exp}}$  should be linear to  $1/H$ , which indeed is the case. From the slope of the  $\chi_{\text{exp}}$  vs  $1/H$  line, we extract  $M_S(\text{Fe}) = 0.14$  emu/g, close to the above estimate of 0.13 emu/g. Assuming this to originate from metallic Fe ( $M_S^\circ = 220$  emu/g), we obtain  $x \approx 0.1$  wt %. Presence of a ferromagnetic impurity (albeit small) naturally influences the overall magnetic moment obtained at 5 K. After deducting the magnetic contribution of 0.1 wt % impurity Fe, an estimate for the correct  $M_S$  value at 5 K for the best-ordered sample with observed  $M_S$  of  $3.96 \mu_B$  is still as high as  $3.94 \mu_B$  assuming no other impurities exist. In case nonmagnetic impurities (e.g.  $\text{SrMoO}_4$ ) are present, the actual  $M_S$  value is certainly no less than  $3.94 \mu_B$ .

We further confirmed the high degree of order by means of  $^{57}\text{Fe}$  Mössbauer spectroscopy for the best-ordered sample. In general the Mössbauer spectra of  $\text{Sr}_2\text{FeMoO}_6$  are completely accounted for using four spectral components.<sup>21,22</sup> The main component, M1, arises from Fe atoms at the correct lattice site. The component originating from Fe atoms occupying the Mo site, i.e. the antisite of Fe, is denoted AS. Furthermore Fe atoms adjacent to the AS atoms, but otherwise at their proper positions, have hyperfine parameters slightly different from those of the M1 atoms and are identified as the third component, denoted M2. The theoretical intensity ratio of 6:1 for the M2 and AS atoms is seen for low concentrations of AS atoms.<sup>22</sup> Finally, Fe atoms residing at antiphase boundaries were recently identified and denoted AP.<sup>21</sup> For component AP very small values of internal field were seen. These four components can be used as starting points also in the analysis of the present spectra.

In Figure 8 the Mössbauer spectra recorded at 77 K for the present sample with  $M_S = 3.96 \mu_B$  are shown. The upper spectrum was recorded at zero applied field, whereas the lower spectrum was obtained in an external field of 600 mT directed perpendicularly to the Mössbauer beam. By visual inspection only two components are resolved from the upper spectrum: M1 and a new (almost) paramagnetic component, denoted SP. In the actual fitting also components M2 and AS were included. Component AS was included in the fit in order to get an estimate of the concentration of antisite Fe based on the Mössbauer data. The possible absence of AS indicates a very low concentration; i.e., only an upper estimate for the concentration of AS Fe can be obtained. The fitted intensity was 1.3%, and judging by the fit curve the concentration is probably smaller. The fitted intensity of M2 was 5%, but this value remains slightly uncertain as the component is located in the outer slopes of component M1. Nevertheless, using the theoretical 6:1 ratio between M2 and AS, an antisite concentration of  $\sim 1\%$  for the Fe atoms is obtained. According to the magnetization data and the Rietveld analysis, the concentration of AS Fe is indeed very low in the sample measured by Mössbauer spectroscopy. For component M1 typical hyperfine parameter values of the  $\text{Fe}^{\text{II/III}}$  state were found: 45.7 T for the internal field and 0.703 mm/s for the isomer shift. The component SP could be

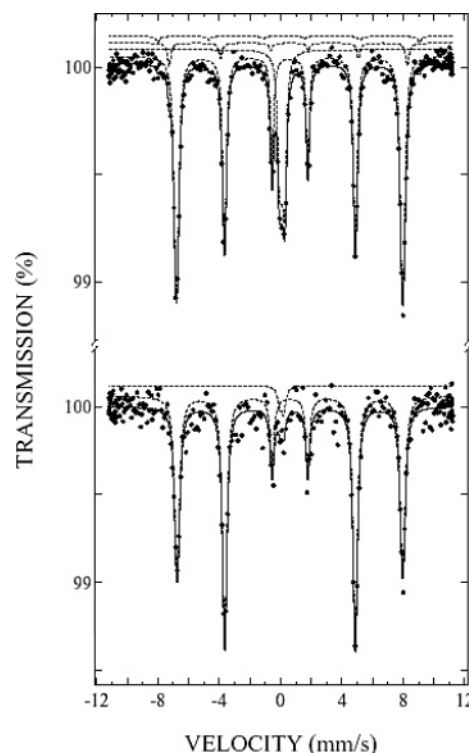


**Figure 8.** Mössbauer spectra for a  $\text{Sr}_2\text{FeMoO}_6$  sample sintered at  $1150^\circ\text{C}$  for 100 h recorded at (a) 77 K, 0 T and (b) 77 K, 600 mT. The upper spectrum exhibits the presence of superparamagnetism, which has been suppressed using an applied field in the lower spectrum. The average angle between the domain magnetization and direction of the beam was fitted to  $79.7^\circ$ . The components used in the fitting are displayed above each spectrum. Reading from the top they are AS, M2, SP, M1 and SP, M1 for the upper and lower spectrum, respectively.

the first glance be interpreted to reflect Fe atoms on antiphase boundaries.<sup>21</sup> However, when the sample was remeasured in an applied magnetic field, the paramagnetic component almost completely disappeared and merged with component M1, suggesting that it has the same origin and that the absence of an internal field was possibly due to super-paramagnetic-type behavior in small sample grains. Note that component AP previously detected for some  $\text{Sr}_2\text{FeMoO}_6$  samples has been found to persist in spectra measured under an applied field of 5 T.<sup>21</sup> To elucidate the origin of component SP, the sample was remeasured in zero applied field at 77 K. Only  $\sim 3\%$  of the original intensity remained; i.e., the intensity transfer to component M1 was irreversible. However, by heating the sample in a vacuum furnace to 445 K (above  $T_C$ ) and again measuring the sample at 77 K and zero applied field, component SP regained a part of its intensity ( $\sim 7\%$ ). By magnetizing the sample, SP could be made to disappear again. At present there is no clear explanation for the presence of component SP. It seems probable that the magnetization of the smallest grains fluctuates easily in the unmagnetized sample, due to the very low coercive force and anisotropy energy. Apparently the magnetization of nearby larger particles does not suffice to pin the magnetization. Upon magnetizing the samples the situation changes as all domains become aligned.

Finally to gain further insight into the magnetic behavior, the temperature dependence of magnetization was measured at 1 T for representative samples having

(21) Lindén, J.; Karppinen, M.; Shimada, T.; Yasukawa, Y.; Yamauchi, H. *Phys. Rev. B* **2003**, *68*, 174415.

(22) Yasukawa, Y.; Lindén, J.; Chan, T. S.; Liu, R. S.; Yamauchi, H.; Karppinen, M. *J. Solid State Chem.* **2004**, *177*, 2655.

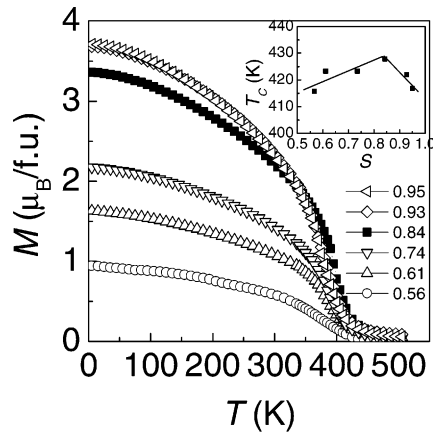


**Figure 9.** Temperature dependence of magnetization at  $H = 1$  T for representative  $\text{Sr}_2\text{FeMoO}_6$  samples having different degrees of order ( $S$ ). Inset shows  $S$  dependence of Curie temperature  $T_C$ .

different  $S$  values. Figure 9 depicts these magnetization curves. We determine Curie temperature  $T_C$  by linear extrapolation of the transition-range data on the  $M$ – $T$  curve to zero magnetization.<sup>6,23</sup> The dependence of  $T_C$  on  $S$  is displayed in the inset of Figure 9. Interestingly, the sample with  $S = 0.84$  exhibits the highest  $T_C$  of 428 K. For  $S < 0.84$ ,  $T_C$  increases with  $S$  along the prediction based on Monte Carlo simulations,<sup>8</sup> whereas  $T_C$  decreases with a further increase in  $S$ . The value of  $T_C$  for the best-ordered sample is 417 K, close to that obtained by the Curie–Weiss law in Figure 7. The effect of Fe/Mo ordering on the Curie temperature has seldom been experimentally investigated, but predictions based on theoretical models have been reported. Monte Carlo simulations assuming superexchange-like interactions between each pair of neighboring cations suggested that  $T_C$  linearly increases with  $S$ .<sup>8</sup> However, a more recent work using a three-band model Hamiltonian led to an increase in  $T_C$  with  $S$  only up to  $S \approx 0.8$ , beyond which the further increase in  $S$  decreased the value of  $T_C$ .<sup>24</sup> Our  $T_C$  data thus are in accordance with the latter prediction. The drop in  $T_C$  within the high- $S$  region is

(23) Navarro, J.; Frontera, C.; Balcels, L.; Martínez, B.; Fontcuberta, J. *Phys. Rev. B* **2001**, *64*, 092411.

(24) Alonso, J. L.; Fernández, L. A.; Guinea, F.; Lesmes, F.; Martín-Mayor, V. *Phys. Rev. B* **2003**, *67*, 214423.

believed to have its origin in the decrease in the ferromagnetic interaction due to the next-nearest-neighbor B-cations (experienced only when the intermediate nonmagnetic Mo between two Fe species is replaced by Fe).<sup>6</sup>

### Conclusion

We have developed a simple and efficient route to prepare high-quality samples of the B-site ordered double-perovskite phase,  $\text{Sr}_2\text{FeMoO}_6$ : a wet-chemical process for the precursor preparation and an encapsulation technique for the sintering are simultaneously used to achieve samples with homogeneous morphology and high degree of B-cation order. The high degree of Fe/Mo order was confirmed from X-ray diffraction, magnetization, and Mössbauer data independently. For the sample sintered at 1150 °C for 100 h, the observed saturation magnetization,  $M_S$ , was as high as  $3.96 \mu_B$ , which is the highest value reported *hitherto*. Application of the wet-chemical process for precursor preparation guarantees that the starting chemicals are mixed in an atomic level and hence makes the precursor powder quite uniform, whereas the encapsulation technique ensures effective reduction by the oxygen getter and keeps the overall cation stoichiometry of the sample stable during the sintering. The combination of these contributions should be responsible for the achieved high degree of order. The present approach can provide a valuable method to synthesize samples of  $\text{Sr}_2\text{FeMoO}_6$  and other similar double-perovskite oxides with high quality.

**Acknowledgment.** We would like to thank Dr. Gang Ni (Institute of Advanced Materials, Fudan University, Shanghai, China) for the magnetic measurements on VSM and Mr. Kim Gustafsson (Physics Department, Åbo Akademi, Finland) for his contribution to the Mössbauer measurements. The present work was supported by Grants-in-Aid for Scientific Research (Nos. 15206002 and 15206071) from the Japan Society for the Promotion of Science. Y.H.H. acknowledges the Japan Society for the Promotion of Science for awarding him the Foreigner Postdoctoral Fellowship (ID P02315). J.L. acknowledges financial support from the Scandinavia-Sasakawa foundation.

CM0493288